THE ASTROPHYSICAL JOURNAL, 409:776–781, 1993 June 1

CHROMOSPHERIC HEATING BY ACOUSTIC SHOCKS: A CONFRONTATION OF GHRS OBSERVATIONS OF α TAURI (K5 III) WITH AB INITIO CALCULATIONS

P. G. JUDGE AND M. CUNTZ[1]
High Altitude Observatory, National Center for Atmospheric Research,[2] 3450 Mitchell Lane, Building 2, Boulder, CO 80301
Received 1992 September 8; accepted 1992 December 1

ABSTRACT

We compare ab initio calculations of C II] line profiles near 2325 Å with recently published observations of the inactive red giant α Tau (K5 III) obtained using the GHRS on board the *Hubble Space Telescope*. Our one-dimensional, time-dependent calculations assume that the chromosphere is heated by stochastic acoustic shocks generated by photospheric convection. We calculate various models using results from traditional (mixing length) convection zone calculations as input to hydrodynamical models.

The C II] line profiles and ratios provide sensitive diagnostics of chromospheric velocity fields, electron densities, and temperatures. We identify major differences between observed and computed line profiles which are related to basic gas dynamics and which are probably not due to technical modeling restrictions. If the GHRS observations are representative of chromospheric conditions at all epochs, then one (or more) of our model assumptions must be incorrect. We suggest the following possibilities: (i) the convection zone has acoustical properties substantially different from those of traditional models, (ii) the atmospheric structure is determined by three-dimensional turbulence and/or horizontal flows not included in our models, (iii) acoustic shocks are not responsible for heating chromospheres of inactive "basal flux" giant stars.

We predict time variability of C II] lines for comparison with observations. Based upon data from the *IUE* archives, we argue that photospheric motions associated with supergranulation or global pulsation modes are unimportant in heating the chromosphere of α Tau. Granule-scale motions would produce variations of a ±few percent on time scales $\sim 2 \times 10^5$ s (2–3 days). Such variations are consistent with existing *IUE* data, but further data are needed.

Subject headings: line: profiles — shock waves — stars: chromospheres — stars: giant — stars: individual (α Tauri)

1. INTRODUCTION

An important outstanding problem in stellar astrophysics concerns the identification of processes responsible for heating stellar chromospheres and coronae. Major advances made during the past 15 yr have led workers to conclude that during main-sequence evolution, low- and intermediate-mass stars possess outer layers whose properties are dominated by magnetic fields (e.g., Zwaan 1991). However, as a single star evolves up the giant branch, magnetic activity subsides, and some researchers (e.g., Schrijver 1987; Rutten et al. 1991) have suggested that nonmagnetic processes control the chromospheric structure of slowly rotating stars later than spectral type K0 III.

These stars present us with an opportunity to study the acoustic chromospheric heating mechanism, which has recently received considerable attention as a heating mechanism for intranetwork regions of the solar chromosphere (e.g., Carlsson & Stein 1991, 1992a, b; Kalkofen 1991). α Tau (K5 III) is a good subject to study, since high-quality echelle data from the Goddard High-Resolution Spectrograph (GHRS) on board the *Hubble Space Telescope* of chromospheric lines have been published (Carpenter et al. 1991). These data include C II] lines between the $2s2p\ ^2P^o$ and $2s2p^2\ ^4P$ terms which provide sensitive diagnostics of chromospheric velocity fields, electron densities, and temperatures (Stencel et al. 1981; Judge 1986).

In this paper, we present a first comparison between fully resolved stellar line profiles and profiles computed from time-dependent, ab initio atmospheric models. These models, used as input to a radiative transfer program, were computed from the response of the outer atmosphere to "realistic" convective motions considering results given by Bohn (1981, 1984). In later work we will report on more detailed properties of these calculations.

2. SPECTRUM CALCULATIONS

Ideally, one should solve self-consistently the coupled equations of gas dynamics and radiative transfer, since these are strongly coupled in chromospheric plasmas (e.g., Carlsson & Stein 1991, 1992a, b). Realistically, such a treatment is not yet possible owing to computational problems involving the treatment of almost coherent scattering in strong resonance lines (e.g., H Lyα) in moving atmospheres. Furthermore, the chromospheres are known to be inhomogeneous (e.g., Wiedemann & Ayres 1990) and such detailed comparisons of stellar observations and theory in homogeneous models are not yet warranted. We therefore made the following simplifications. First, we solved the hydrodynamic and thermodynamic equations, using an approximate treatment of radiative transfer effects for hydrogen. Second, we used these solutions as input to an accurate radiative transfer program with which we calculated spectra of C II] lines for comparison with observations.

2.1. *Hydrodynamical Calculations*

We used a modified version of the code described by Cuntz & Ulmschneider (1988), which solves the equations of hydro-

[1] Joint Institute for Laboratory Astrophysics, University of Colorado and National Institute of Standards and Technology, Boulder, CO 80309-0440.

[2] The National Center for Atmospheric Research is sponsored by the National Science Foundation.

dynamics for radiating flows using the method of characteristics. The most important assumptions and approximations influencing our solutions include:

1. Shock waves with a sawtooth profile were inserted at the inner boundary. Thus, we assumed that shocks had already formed at lower heights (e.g., Ulmschneider 1989). The outer boundary was assumed to be transmitting, and the shocks were treated as discontinuities.

2. The wave periods were changed stochastically keeping the wave amplitudes constant. Bohn (1981, 1984) computed a grid of stellar convection zone models for different late-type stars using the mixing-length concept. He derived acoustic energy fluxes and wave periods associated with the convective motions. We adopted the wave period having the highest energy flux in Bohn's model as the period of the peak value in a stochastic period distribution. (This assumption is therefore different from approaches based upon a "white noise" spectrum of wave periods).

3. Radiation transport in lines and continua of hydrogen were treated in an approximate non–LTE approach including a two-level atom plus continuum. Following Hartmann & Avrett (1984), Lyα was approximated using the local escape probability approximation, and escape probabilities were set to $1/(1 + \tau_0)$ where τ_0 is the line center optical depth. Thus, no nonlocal transfer of radiation was treated. We used static escape probabilities since velocity gradients outside the shock discontinuities were much less than in the Sobolev limit.

4. The ionization balance of hydrogen was determined by setting the Lyman continuum in radiative detailed balance (e.g., Hartmann & Avrett 1984). Thus, the rates determining the ionization balance of hydrogen include photoionization and radiative recombination in the Balmer continuum (a radiation temperature of 2847 K was adopted in the chromosphere [Ayres 1975]) and collisional ionization from the $n = 1$ and $n = 2$ levels. These calculations were included consistently in the hydrodynamic and thermodynamic equations including the Rankine-Hugoniot relations.

5. All rates in the statistical equilibrium equations were assumed to be much faster than rates at which thermodynamical quantities change. Thus the time derivative and advective terms in the rate equations were set to zero.

6. Radiation losses were treated using the effectively thin rates of Judge & Neff (1990), which also implicitly assume (5). Loses in H Lyα are negligible in comparison with losses from Ca II, Mg II, and Fe II lines since the calculated temperatures never exceed $\sim$7000 K.

Our procedure for constructing dynamical models went as follows. First, we adopted estimates of fundamental stellar data (Table 1) and constructed a hydrostatic atmosphere at a temperature near 3000 K. The gas density at the lower boundary was taken from densities near the temperature minimum region of the model atmosphere of α Tau of Kelch et al. (1978). Next, we introduced perturbations at the lower boundary with a monochromatic wave of period $P_{\rm Peak} = P_c/10$ ($= 3.5 \times 10^4$ s) for 10^5 s (the sound crossing time of our computational domain is 3×10^5 s). P_c is the acoustic cutoff period near the top of the convection zone (Table 1). Finally, we introduced perturbations having a Gaussian probability distribution of wave periods centered at $P_c/10$ with both narrow and wide bandwidths σ_P (Table 2), omitting negative periods. Since our aim is to study line profiles for comparison with observations, these parameters were chosen to correspond to those of convection zone models available. The amplitudes of the perturbations were chosen so that the wave energy flux densities F_0 (ergs cm^{-2} s^{-1}) span the observed estimate of the total chromospheric radiative flux density $F_{\rm chrom}$ given by Judge & Stencel (1991, see Table 1). Four models were computed (Table 2).

TABLE 1

ADOPTED STELLAR PARAMETERS FOR α TAURI

Parameter		Value
$T_{\rm eff}$		3970 K
log g		1.3 cm s^{-2}
P_c	(Acoustic cutoff period)	3.5×10^5 s
T_R(Ba $-$ κ)	(Radiation temperature)	2847 K
C abundance	(Logarithmic scale, $H \equiv 12$)	8.38
$F_{\rm chrom}$	(Nonradiative heating)	2.8×10^5 ergs cm^{-2} s^{-1}

2.2. *Radiative Transfer Calculations*

The hydrodynamical models were used as input to the program MULTI (Carlsson 1986). These models do not extend into photospheric depths owing to restrictions in the treatment of the radiative energy balance in the hydrodynamics code. Therefore, we used the atmospheric model of Kelch et al. (1978) as a base atmosphere at column masses m greater than 0.1 g cm^{-2}. This does not affect our conclusions since the C II] emission-line cores are formed in higher layers. We solved the transfer equation using 75 depth points in the model atmosphere for each time step.

We treated carbon with a 3-level model for C I (the lowest three terms: $2p^2\,{}^3P$, ${}^1D$, ${}^1S$), the lowest seven levels of C II ($2s^2 2p\,{}^2P^0_{1/2,\,3/2}$, $2s2p^2\,{}^4P_{1/2,\,3/2,\,5/2}$, $2s2p^2\,{}^2D_{5/2,\,3/2}$) and the C III ground level ($2s^2\,{}^1S_0$). We included C I and C III as well as C II to permit accurate estimates of the C II number densities at all heights in the atmosphere. The atomic energy levels, oscillator strengths, collision cross sections, and photoionization cross sections are from sources listed by Judge (1986). Newer calculations by Blum & Pradhan (1992) give almost identical collision strengths to those of Lennon et al. (1985) used here. We adapted oscillator strengths from Lennon et al. (1985). We used 50 frequency quadrature points for each C II] line. We enhanced background opacities by a factor of 2 at near-ultraviolet wavelengths to mimic the effects of missing line opacity. This produced a more realistic background opacity at the wavelengths of the C II] lines.

3. COMPARISON OF COMPUTED AND OBSERVED LINE PROFILES

Our primary results are summarized in Figures 1 and 2 and in Table 3. Figure 1 shows properties of one dynamical model and computed C II] spectra for one time step, together with the time-averaged atmosphere and spectra, and observed spectra

TABLE 2

INPUT WAVE PROPERTIES

Run	F_0 (ergs cm^{-2} s^{-1})	$P_{\rm Peak}$ (s)	σ_P (s)	$\int dt$[a] (s)
1	7.8×10^4	3.5×10^4	5.25×10^4	1.1×10^6
2	8.3×10^4	3.5×10^4	10.5×10^4	9.6×10^5
3	8.4×10^5	3.5×10^4	5.25×10^4	9.9×10^5
4	1.0×10^6	3.5×10^4	10.5×10^4	9.1×10^5

[a] $\int dt$ is the time interval over which our calculations were made. The sound crossing time for the computational domain is roughly 3×10^5 s.

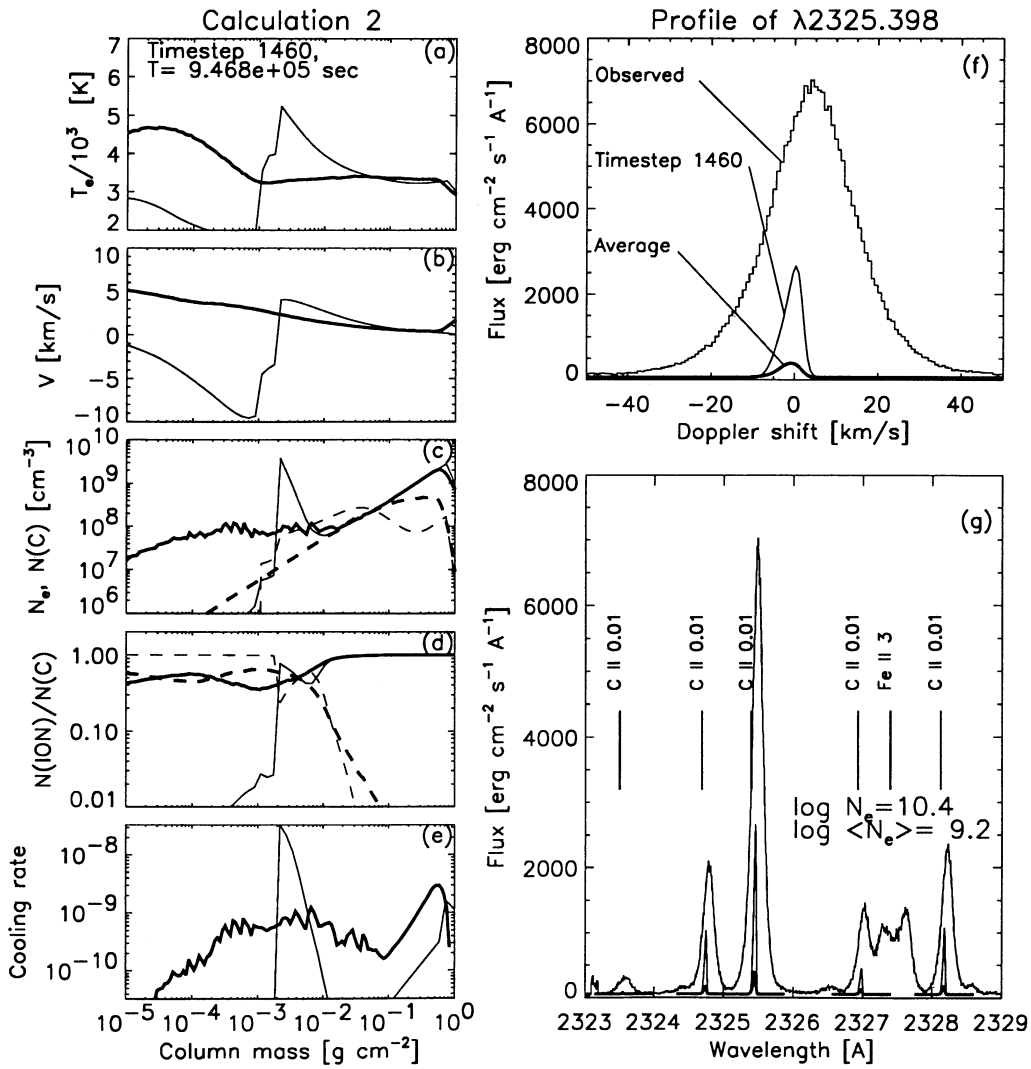

FIG. 1.—Computed shock model and line profiles for one time-step (*thin solid lines*) and time-averaged data (*thick lines*). Also shown are spectra from the echelle mode of the GHRS on the *Hubble Space Telescope* (*histograms*). The panels show (*a*) electron temperatures, (*b*) velocities (the solid line is the rms time-averaged velocity), (*c*) electron densities (*solid lines*) and carbon densities (*dashed lines*), (*d*) ionization fractions of C I (*solid*) and C II (*dashed*), (*e*) the cooling rate of the λ2325.398 line of C II, (*f*) the profile of λ2325.398, (*g*) the λ2323–λ2329 region together with electron densities derived from the computed line ratios (see text).

TABLE 3

CALCULATED C II] LINE PROFILE PARAMETERS

Run	$\langle F \rangle$ (ergs cm^{-2} s^{-1})	$\langle$FWHM$\rangle$ (km s^{-1})	$\langle V \rangle$ (km s^{-1})	$\langle N_e \rangle$ (cm^{-3})	$\sigma(F)/\langle F \rangle$	$\sigma(F^g)/\langle F \rangle$
1	12.5	4.8	−1.4	9.0	1.1	0.05
2	16.7	5.1	−1.2	9.2	1.8	0.07
3	71.8	4.5	−1.9	9.2	0.9	0.05
4	87.0	4.8	−2.1	9.3	1.6	0.07
Observed	1360	24 ± 3	+3.9 ± 0.4	9.0 ± 0.1	...	...

Parameters refer to the λ2325.398 line, except for the values of $\langle N_e \rangle$ which are electron densities derived from the ratios R_1, R_2, and R_3 (Stencel et al. 1981; Lennon et al. 1985) of the time-averaged calculated flux densities of four of the C II] lines. The observed data are from Carpenter et al. 1991. $\sigma(F)/\langle F \rangle$ is the standard deviation of the time-dependent flux density divided by the time-averaged flux. $\sigma(F^g)/\langle F \rangle$ is the same quantity except that $\sigma(F^g)$ was calculated from a randomized sum of 500 individual time series (see text).

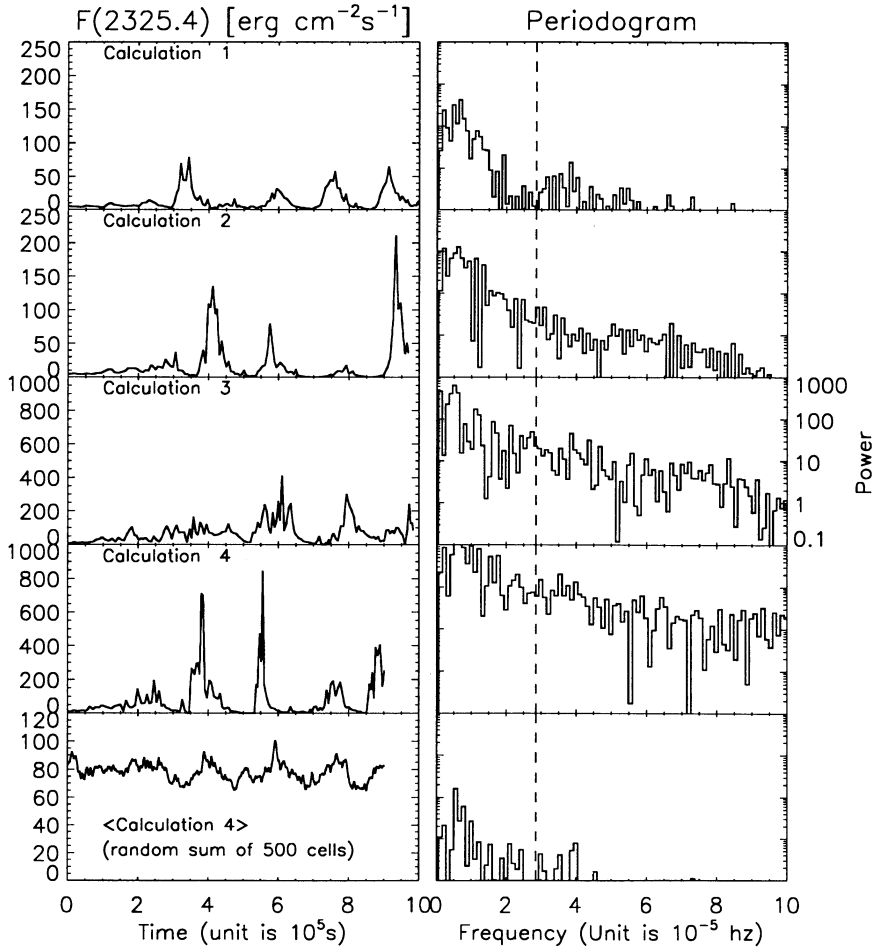

FIG. 2.—Time variations and periodograms of the integrated flux density $\int F_\lambda d\lambda$ of the λ2325.398 line for all four hydrodynamical models. The dashed line in the periodogram is the peak frequency at which power was input at the atmospheric base in all models. The bottom panel shows the time dependence of an ensemble of 500 model 4 calculations, excited at random phases. This represents the predicted time behavior of the C II line flux if the chromosphere of α Tau is heated by 500 independently operating "pistons," the expected number of granule cells visible on the star's hemisphere (see text).

from echelle spectrograph of the GHRS. Typically there are just one or two shocks at a given time in the regions where the C II] lines are formed (at column masses between 10^{-4} and 10^{-1} g cm^{-2}). The formation of the C II] lines is essentially restricted to a narrow layer in the post-shock regions, as illustrated by the cooling rate of the C II] λ2325.4 line. (For optically thin emission lines, the contribution function for frequency-integrated emergent flux corresponds to the cooling function [Judge 1990]).

We recognize that at each time step, these calculations represent a limiting case where the atmospheric properties at each height are pulsating coherenty. This is inconsistent with our input spectra of waves, which were assumed to be generated by small-scale convective motions. Therefore, we must invoke the *ergodic hypothesis* and assume that the *time* averages of our homogeneous one-dimensional calculations are equivalent to the *spatial* averages of the inhomogeneous stellar chromosphere when observed at given times. In computing time averages and relating these to spatial averages, we ignore limb darkening and limb projection effects.

3.1. *Time-averaged Calculations versus Observed Profiles*

Let the time average of a quantity x be $\langle x \rangle$. The time-averaged results shown in Figure 1 and Table 3 can be summarized as follows. (i) The computed line widths $\langle$FWHM$\rangle$ are factors of $\sim$4 smaller than the observed line widths. (ii) The centroid of the computed emission profiles $\langle V \rangle$ are *blueshifted* by $\sim$1–2 km s^{-1}, whereas the observed profiles are *redshifted* by 3.9 $\pm$ 0.4 km s^{-1}. (iii) The computed emergent flux densities $\langle F \rangle$ increase with increasing input wave flux density F_0, but they are between 1 and 2 orders of magnitude less than observed. $\langle F \rangle$ also increases (weakly) with the width of the adopted frequency spectrum. (iv) The computed ratios of the frequency-integrated flux densities of the lines can be used to "measure" the electron densities in the same way that the observed data can (Stencel et al. 1981). These yield values in good agreement with those observed (but see § 4.1). The interpretation and consequences of these results are discussed below.

3.2. *Time-Dependent Spectral Properties of Shock-heated Chromospheres*

Figure 2 shows the time dependence of the integrated flux density F(2325.4) of the strongest line of the C II] multiplet at 2325.4 Å, for the four calculations. Also shown are periodograms of these data (with the means removed). The first 10^5 s of all calculations were uneventful, since shock merging did not occur (the wave input spectrum was monochromatic). At later

times the stochastic input spectrum generated enormous variations in $F(2325.4)$, as measured by the large standard deviations $\sigma(F)$. The quantity $\sigma(F)/\langle F\rangle$ increased substantially for the "wide" input wave spectra. Most of the variations occurred at wave periods between $P_{\rm Peak}$ and P_C.

These effects are due to two physical properties: (i) the C II] lines are formed primarily behind shocks, and (ii) strong shocks (with high Mach numbers) overtake and "cannibalize" weaker shocks, transferring wave power from small to large geometrical scales (Cuntz 1987; 1992). The emissivity ϵ_ν (ergs cm^{-3} s^{-1} Hz^{-1} sr^{-1}) of the C II] lines at frequencies ν depends strongly on the number density $N_{\rm C\,II}$, on electron density N_e, and temperature T_e: $\epsilon_\nu \propto N_{\rm C\,II}\ N_e \exp(-h\nu/kT_e)/(T_e)^{1/2}$. Only the strongest and by implication least frequently formed shocks have high enough values of N_e and T_e deep enough in the model (i.e., high $N_{\rm C\,II}$) to contribute significantly to ϵ_ν and F. Thus, if chromospheres of cool giant stars are heated by shock waves of the type considered here, then enormous changes in the intensity of UV lines like C II] would be (locally) produced. However, if small structures (e.g., granules) are the source of the shock waves considered here, then an *ensemble* of such calculations is needed to make sensible comparisons with observations.

3.3. *Time-dependent Signatures of Global Pulsation, Supergranulation, Granulation*

Variability of the type shown in the top eight panels of Figure 2 has never been observed in chromospheric lines of K giant stars. We noted above that these computations represent unrealistic limits to the predicted variability of $F(2325.4)$, unless the entire atmosphere is pulsating or convecting in coherent (i.e., low-order) modes. K giants show low-amplitude (just tens of meters sec^{-1}) radial velocity variations in photospheric lines (e.g., Smith et al. 1987, Cochran 1988, Walker et al. 1989, Belmonte et al. 1990).

We now ask on what lateral scales the convective motions might occur on α Tau. Unfortunately, little is known empirically about convection in giant stars. Based upon observed properties of solar convection and theoretical arguments, Schwarzschild (1975) and Antia, Chitre, & Narasimha (1984) argued that the convective cells of cool, low-gravity stars might be much larger than the Sun (when expressed as a fraction of a stellar radius). For α Tau, Schwarzschild's scalings predict a total of $\sim$500 granules and just $\sim$2 supergranules on the visible hemisphere. Immediately we see that the source of chromospheric heating, if acoustic, cannot be coherent on supergranule scales envisaged by Schwarzschild since this would predict variations similar to those shown in the upper panels of Figure 2. The variability of chromospheric lines of α Tau is at most a few percent, judging from existing *IUE* observations (Judge & Jordan 1991).

The two bottom panels of Figure 2 show a time series and periodogram of F^g, where $F^g(t) = \frac{1}{500}\{\sum_{j=1}^{500} F_j(t-\phi_j T)\}$, where ϕ_j is a random phase between 0 and 1, $F(t)$ is the computed flux density at time t, and T is the total integrated time span of the time series of $F(t)$ [$F(t)$ was assumed to be periodic with period T]. $F^g(t)$ therefore represents the randomized sum of 500 "cells" visible on the star's hemisphere. (Solar granulation shows little correlation between individual granule cells [Title et al. 1989]).

Based upon these data, we make the following predictions. *If the chromosphere of α Tau is heated by acoustic waves generated by granules, then time series observations of optically thin lines such as* C II *λ2325.4 will have peak power at frequencies near* 0.5×10^{-5} Hz *(periods near* 2–3 *days), and amplitudes determined primarily by the number of visible granules. For* 500 *granules, the* 1 *σ amplitudes are expected to be near* 5% (Table 3, last column). Such amplitudes should be detectable with the *IUE* satellite (e.g., Ayres 1984).

4. DISCUSSION

Our calculations reveal major differences between computed and observed GHRS line profiles of C II] lines. What can we conclude from these differences?

4.1. *Qualitative Implications of Our Assumptions*

There are important consequences of our assumptions which will influence some of our results. (i) Nonlocal radiative transfer in optically thick lines of hydrogen will smooth out discontinuities in number densities of H atoms, protons, and electrons (e.g., Kalkofen & Whitney 1971). Our local approximation maximizes changes in proton densities and hence electron densities across shocks. (ii) Time derivative and advection terms in the statistical equilibrium equations will drive atomic number densities away from static equilibrium values.

Nonlocal transfer in hydrogen lines will substantially alter the ionization structure and electron density near the shock. It is possible that the preshock (inflowing) gas could be strongly ionized even though the local kinetic temperature is very low. This would enhance C II] emission from these regions. However, gas densities are much lower in these inflowing regions (Fig. 1) and little contribution to the total emergent intensity would be expected from the inflowing gas. Hence, a net redshift of the C II] lines cannot be produced by this effect.

An improved treatment of the statistical equilibrium equations will lead to two effects: First, the gas thermodynamics will differ in regions close to shocks, since it is dominated by the behavior of hydrogen (the dominant atmospheric constituent and source of chromospheric electrons). Carlsson & Stein (1991, 1992a, b) showed that, in the solar chromosphere, temperature differences across shocks can be increased by a net radiative heating in cases where recombination rates are small in comparison with dynamical rates of change. Second, the formation of the C II] lines will be influenced by these changes in shock structure and by the time derivative and advection terms themselves. In our calculations carbon is mostly singly ionized at column densities below 10^{-2} g cm^{-2} by photoionization in the C I continua (C III is negligible). We therefore expect to see changes in the ionization balance of C I/C II, and in the collisional excitation rates of the intersystem lines. These will act on the line emissivities in opposite senses since more C II relative to C I behind the shocks will result from the former, and less electron collisional excitation will result from the latter.

However, we expect that some properties of our calculations will remain largely unaltered by relaxation of these assumptions: the strengths and speeds of the shocks, the gas speeds on both sides of the shocks, and as a consequence C II] *line profiles.* The primary influences of these assumptions in the gas dynamic equations occur through the treatments of radiation losses and of the equation of state. These primarily affect the energy equation, but the momentum equation remains largely unaffected. This statement has support from numerical calculations which compare shock strengths from models with different treatments of radiative losses (e.g., Schmitz, Ulmschneider, & Kalkofen 1985). The only term in the momentum equation directly affected is the thermal pressure gradient, which is negligible in comparison with wave pressure initiated by the shocks. We conclude that although we cannot trust our com-

puted temperatures, electron densities, and hence line intensities without additional work, the shapes of the line profiles are not expected to change drastically when a more accurate treatment of shock structures is considered. Therefore, we believe that a set of robust conclusions can be presented which is independent of the technical restrictions of the models.

4.2. "*Robust*" *Conclusions*

1. Outwardly propagating, one-dimensional shock waves generated using input waves with realistic energy fluxes and reasonable frequency spectra fail to account for the gas dynamics as inferred from the GHRS observations.

2. We presented arguments which indicate that redshifted emission lines are impossible to reproduce in these models.

3. The chromosphere of α Tau is much more turbulent than our calculations can produce. Similarly, Carlsson & Stein (1992a, b) needed to include "microturbulence" in their one-dimensional calculations to obtain realistic profiles of Ca II *H* and *K* lines.

4. A comparison of observed and computed C II] energy fluxes and derived electron densities is not yet possible owing to our assumptions which yield incorrect values of electron temperatures and densities behind shocks.

5. If the chromosphere is heated by the action of acoustic waves, the souces of the waves cannot be coherent on supergranule scales since this would predict large C II] variability, which has not been observed. This mechanism also predicts that time series observations will reveal periodicities near 2–3 days and amplitudes ±a few percent (for 500 cells). The amplitudes will be determined by the number of convective cells on the star.

4.3. *Speculations and Suggestions for Future Work*

Work is in progress to relax our assumption of static statistical equilibrium in the hydrogen rate equations. However, the gross disagreements between theoretical and observed velocity fields already suggest interesting possibilities. The observed net redshift is small in comparison with the observed turbulence (Table 3). Thus, it appears likely that the star always shows the observed net redshift, since even if the observations were obtained at an epoch when the star was suffering a large-scale downflow (accretion shock), small-scale velocity fields are more important in the gas dynamics. Furthermore, the redshift does not occur for all chromospheric lines (Carpenter et al. 1991). Only additional observations with the GHRS can show if the observed redshift was caused by an unusual large-scale event, or whether it is a "permanent" property of the chromosphere of α Tau.

A steady state downflow might be related to the solar phenomenon in which lines formed at transition region temperatures show systematic downflows relative to chromospheric lines (e.g., Hassler, Rottman, & Orral 1991). This phenomenon has also been observed in active late-type stars (Ayres, Jensen, & Engvold 1988). Although the cause of this is not yet understood (Hansteen 1993), it seems to require magnetic fields at least to channel the fluid flow, if not actually to drive the flow. Much remains to be learned about the role of magnetic activity in late phases of stellar evolution. Further simultaneous observations of the UV lines (including C II]) and of plasma at lower temperatures (e.g., CO lines, Wiedemann & Ayres 1990) and higher temperatures (e.g., He I λ10830, O'Brien & Lambert 1986) should provide important additional clues.

Finally, if magnetic activity does not play a major role in α Tau, our work might indicate that either the convection zone in α Tau has acoustical properties substantially different from those of traditional mixing length models, or the atmospheric structure is determined by three-dimensional turbulence and/or horizontal flows. Theoretical evidence for these possibilities has been presented by Malagoli, Cattaneo, & Brummell (1990) and Dravins et al. (1993) and references therein.

We thank J. Linsky, K. MacGregor, and V. Hansteen for comments on an early version of the manuscript, and M. Carlsson for copies of papers prior to publication. M. C. acknowledges financial support through the Advanced Study Program at the National Center for Atmospheric Research and by the National Aeronautics and Space Administration (grants NAG 5-1374 and NAG W-2904 to the University of Colorado).

REFERENCES

Antia, H. M., Chitre, S. M., & Narasimha, D. 1984, ApJ, 282, 574
Ayres, T. R. 1975, Ph.D. thesis, Univ. Colorado
———. 1984, ApJ, 284, 784
Ayres, T. R., Jensen, E., & Engvold, O. 1988, ApJS, 66, 51
Belmonte, J. A., Jones, A. R., Pallé, P. L., & Cortés, T. R. 1990, ApJ, 358, 595
Blum, R. D., & Pradhan, A. K. 1992, ApJS, 80, 425
Bohn, H. U. 1981, Ph.D. thesis, Univ. Würzburg
———. 1984, A&A, 136, 338
Carlsson, M. 1986, Uppsala Obs. Rep. 33
Carlsson, M., & Stein, R. F. 1991, Mechanisms of Chromospheric and Coronal Heating, ed. P. Ulmschneider, E. R. Priest, & R. Rosner (Berlin: Springer), 366
———. 1992a, in Seventh Cambridge Workshop on Cool Stars, Stellar Systems, and the Sun, ed. M. S. Giampapa & J. A. Bookbinder (PASP Conf. Series 26), 515
———. 1992b, ApJ, 397, L59
Carpenter, K. G., Robinson, R. D., Wahlgren, G. M., Ake, T. B., Ebbets, D. C., Linsky, J. L., Brown, A., & Walter, F. M. 1991, ApJ, 377, L45
Cochrane, W. D. 1988, ApJ, 334, 349
Cuntz, M. 1987, A&A, 188, L5
———. 1992, in Seventh Cambridge Workshop on Cool Stars, Stellar Systems, and the Sun, ed. M. S. Giampapa & J. A. Bookbinder (PASP Conf. Series 26), 383
Cuntz, M., & Ulmschneider, P. 1988, A&A, 193, 119
Dravins, D., Lindegren, L., Nordlund, Å., & VandenBerg, D. A. 1993, ApJ, 403, 385
Hansteen, V. 1993, ApJ, 402, 741
Hartmann, L., & Avrett, E. H. 1984, ApJ, 284, 238
Hassler, D. M., Rottman, G. S., & Orral, F. Q. 1991, ApJ, 372, 710
Judge, P. G. 1986, MNRAS, 221, 119
Judge, P. G. 1990, ApJ, 348, 279
Judge, P. G., & Jordan, C. 1991, ApJS, 77, 75
Judge, P. G., & Neff, D. H. 1990, in Sixth Cambridge Workshop on Cool Stars, Stellar Systems and the Sun, ed. G. Wallertein (PASP Conf. Series 9), 57
Judge, P. G., & Stencel, R. E. 1991, ApJ, 371, 357
Kalkofen, W. 1991, in Solar Interior and Atmosphere, ed. A. N. Cox, W. C. Livingstone, & M. S. Matthews (Tucson: Univ. Arizona Press), 911
Kalkofen, W., & Whitney, C. A. 1971, JQSRT, 11, 531
Kelch, W. L., Linsky, J. L., Basri, G. S., Chiu, H., Chang, S., Maran, S. P., & Furenlid, I. 1978, ApJ, 220, 962
Lennon, D. J., Dufton, P. L., Hibbert, A., & Kingston, A. E. 1985, ApJ, 294, 200
Malagoli, A., Cattaneo, F., & Brummell, N. H. 1990, ApJ, 361, L33
O'Brien, G. T., & Lambert, D. L. 1986, ApJS, 62, 899
Rutten, R. G. M., Schrijver, C. J., Lemmens, A. F. P., & Zwaan, C. 1991, A&A, 252, 203
Schmitz, F., Ulmschneider, P., & Kalkofen, W. 1985, A&A, 148, 217
Schrijver, C. J. 1987, A&A, 172, 111
Schwarzschild, M. 1975, ApJ, 195, 137
Smith, P. H., McMillan, R. S., & Merline, W. J. 1987, ApJ, 317, L79
Stencel, R. E., Linsky, J. L., Brown, A., Jordan, C., Carpenter, K. G., Wing, R. F., & Czyzak, S. 1981, MNRAS, 196, 47P
Title, A. M., Tarbell, T. D., Topka, K. P., Ferguson, S. H., Shine, R. A., and the SOUP Team. 1989, ApJ, 336, 475
Ulmschneider, P. 1989, A&A, 222, 171
Walker, G. A. H., Yang, S., Campbell, B., & Irwin, A. W. 1989, ApJ, 343, L21
Wiedemann, G., & Ayres, T. R. 1990, in Sixth Cambridge Workshop on Cool Stars, Stellar Systems, and the Sun, ed. G. Wallerstein (PASP Conf. Ser. 9), 158
Zwaan, C. 1991, in Mechanisms of Chromospheric and Coronal Heating, ed. P. Ulmschneider, E. R. Priest, & R. Rosner (Berlin: Springer), 241